Autosomal-Dominant Striatal Degeneration Is Caused by a Mutation in the Phosphodiesterase 8B Gene

Silke Appenzeller,[1,9] Anja Schirmacher,[2,9] Hartmut Halfter,[2] Sebastian Bäumer,[2] Manuela Pendziwiat,[2] Vincent Timmerman,[3] Peter De Jonghe,[3] Klára Fekete,[4] Florian Stögbauer,[5] Peter Lüdemann,[6] Margret Hund,[7] Elgar Susanne Quabius,[8] E. Bernd Ringelstein,[2] and Gregor Kuhlenbäumer[1,*]

Autosomal-dominant striatal degeneration (ADSD) is an autosomal-dominant movement disorder affecting the striatal part of the basal ganglia. ADSD is characterized by bradykinesia, dysarthria, and muscle rigidity. These symptoms resemble idiopathic Parkinson disease, but tremor is not present. Using genetic linkage analysis, we have mapped the causative genetic defect to a 3.25 megabase candidate region on chromosome 5q13.3-q14.1. A maximum LOD score of 4.1 ($\Theta = 0$) was obtained at marker D5S1962. Here we show that ADSD is caused by a complex frameshift mutation (c.94G>C+c.95delT) in the phosphodiesterase 8B (*PDE8B*) gene, which results in a loss of enzymatic phosphodiesterase activity. We found that *PDE8B* is highly expressed in the brain, especially in the putamen, which is affected by ADSD. PDE8B degrades cyclic AMP, a second messenger implied in dopamine signaling. Dopamine is one of the main neurotransmitters involved in movement control and is deficient in Parkinson disease. We believe that the functional analysis of *PDE8B* will help to further elucidate the pathomechanism of ADSD as well as contribute to a better understanding of movement disorders.

Autosomal-dominant striatal degeneration (ADSD [MIM 609161]) is a rare autosomal-dominant disease affecting the striatal part of the basal ganglia.[1] The main clinical features of ADSD are slowly progressive dysarthria, bradykinesia presenting predominantly as gait disturbance, and muscle rigidity as well as diadochokinesis. Tremor is not present. In contrast to Parkinson disease (PD [MIM 168600]), the patients do not show a good response to L-Dopa therapy. The age of onset of clinical symptoms is in the fourth to fifth decade, with no apparent reduction in life expectancy. Brain MRIs show distinctive lesions of the striatum (putamen, caudate nucleus, and nucleus accumbens) appearing earlier than the onset of symptoms. MRI abnormalities consist primarily of a signal increase on T2-weighted images (Figure 1A) and a corresponding signal decrease on T1-weighted images.[1]

To identify the gene underlying the ADSD phenotype in an ADSD family, we followed a classical linkage-analysis approach. Seventeen members of a German ADSD family (Figure 1B) underwent neurologic examination and received T1- and T2-weighted spin-echo MRI examinations at 1.5 Tesla.[1] DNA was isolated from white blood cells via standard protocols. Seventeen individuals, seven of whom are affected, were included in the initial genome scan and the fine mapping as described previously.[1] The study was approved by the ethics committee of the University of Muenster, Germany, and informed consent was obtained. We mapped ADSD to a 3.25 Mb candidate region on chromosome 5q13.3-14.1 by genome-wide linkage analysis (see Tables S1 and S2 available online). A maximum LOD score of 4.1 ($\Theta = 0$) was obtained at marker D5S1962. Analysis of 34 additional short tandem repeat (STR) markers within the candidate region with an average intermarker distance of 70 kb did not allow further reduction of the candidate region (Table S2). Primer sequences for the STR markers used in the delineation of the candidate region are listed in Table S3. PCR conditions are available upon request.

STR markers did not show triple alleles or hemizygosity, arguing against large duplications or deletions causing ADSD (data not shown).

The candidate region contained 21 known RefSeq annotated protein-coding genes (Figure 2A). Positional candidate genes were obtained from the RefSeq database with the UCSC Human Genome Browser (hg18). Coding exons and intronic flanking regions of all protein coding genes in the candidate region were analyzed for sequence variations by direct DNA sequencing. Sequences included about 30–100 base pairs (bp) of intronic sequence for detection of splice-site mutations. Primer sequences were based on the reference sequence of each gene deposited in RefSeq. Primer sequences for the phosphodiesterase 8B gene (*PDE8B* [MIM 603390]) are given in Table S4. The genomic structure of *PDE8B* is shown in Figure 2B. Sequence analysis was performed with the BigDye Terminator Cycle Sequencing Kit v3.1 (Applied Biosystems), and products were run on

[1]Department of Molecular Neurobiology, Institute of Experimental Medicine, University of Kiel, Kiel 24105, Germany; [2]Department of Neurology, University of Münster, Münster 48149, Germany; [3]Department of Molecular Genetics, VIB and University of Antwerpen, Antwerpen 2610, Belgium; [4]Department of Neurology, University of Debrecen, Debrecen 4012, Hungary; [5]Department of Neurology, Klinikum Osnabrück, Osnabrück 49076, Germany; [6]St. Franziskus Hospital Ahlen, Ahlen 59227, Germany; [7]Zürcher Höhenklinik Wald, Faltigberg 8639, Switzerland; [8]Department of Immunology, University of Kiel, Kiel 24105, Germany
[9]These authors contributed equally to this work
*Correspondence: g.kuhlenbaeumer@neurologie.uni-kiel.de
DOI 10.1016/j.ajhg.2009.12.003.

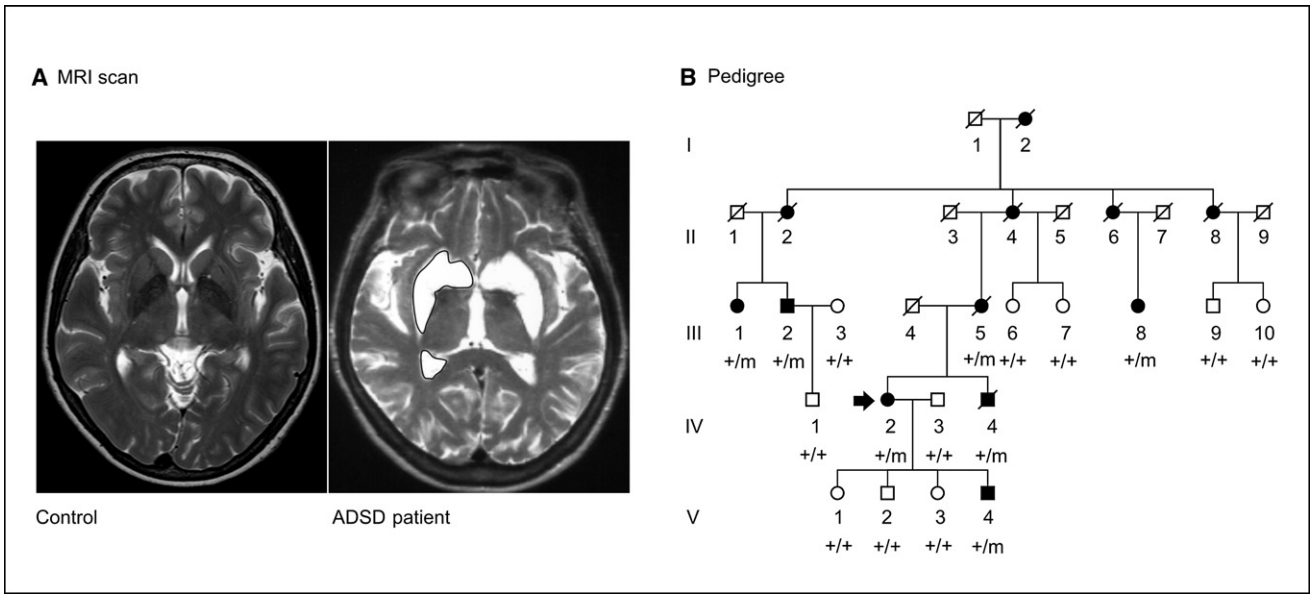

Figure 1. MRI Features and Pedigree of the ADSD Family
(A) T2-weighted images of a healthy control (left) and ADSD patient III:5 (right; encircled are regions of pathologic signal increase).
(B) Pedigree of the ADSD family. Clear symbols represent unaffected individuals. Filled symbols represent individuals with ADSD. Individuals were considered affected on the basis of the characteristic symmetric MRI abnormalities of the basal ganglia. The index patient (IV:2, arrow) is shown in Movie S1. Segregation analysis showed perfect cosegregation of the *PDE8B* mutation (c.94G>C+c.95delT) with ADSD. +/m denotes heterozygous mutation carriers; +/+ denotes individuals homozygous for the wild-type allele.

a 3730 DNA Analyzer (Applied Biosystems) and analyzed with the "Seqman" module from the DNASTAR package (DNASTAR, Inc.). We detected a heterozygote sequence variation (c.94G>C+c.95delT) (Figure 2C) in the first exon of *PDE8B* (NM_003719). Five hundred unrelated healthy controls were analyzed for the ADSD-causing mutation, 200 by direct sequencing and 300 by PCR restriction fragment-length polymorphism. PCR primers were as follows: forward, 5′-CAGAGCGGCGTGATCTACT-3′; and reverse, 5′-GTGTAGCAGGTCTGAGTCTCG-3′. The PCR product of 299 bp (wild-type) or 298 bp (mutant) was digested with the restriction enzyme *OliI* (Fermentas), resulting in two fragments of 61 and 238 bp for the wild-type allele. The PCR product of the mutant allele was not digested by *OliI*. This sequence variation segregates with ADSD and was found neither in the 500 ethnically matched control individuals nor in the sequence-variation database dbSNP. No other potentially ADSD-causing mutation was detected in any of the 21 candidate genes. These results strongly argue that ADSD is caused by the *PDE8B* mutation. However, these data would be strengthened further if a second family with ADSD had been available for the study.

The frameshift mutation alters the amino acid sequence of the PDE8B protein C terminus of amino acid 31 and introduces a premature stop after 63 amino acids (NM_003719) (Figures 2E and 2F). Phosphodiesterases (PDEs) regulate the localization, duration, and amplitude of cyclic nucleotide signaling within subcellular compartments. The intracellular levels of cyclic AMP (cAMP) and cyclic guanosine monophosphate (cGMP) are controlled by their rates of synthesis as well as by their rates of degradation by phosphodiesterases. Eleven distinct PDE protein families have been described in humans.[2] All PDEs share a conserved C-terminal catalytic region but have highly variable N termini composed of different domains that presumably confer distinct regulatory properties to the individual PDE families.[2] The conserved PDE catalytic domain is composed of 270–300 amino acids located in the C-terminal part of each PDE.[3] PDE8B is a cAMP-specific isobutyl-1-methylxanthine (IBMX)-insensitive phosphodiesterase that catalyzes the hydrolysis of the second messenger 3′,5′-cAMP to 5′-AMP.[3] *PDE8B* is composed of 23 exons.[4,5] Six alternative splice variants are known (Figure 2B; Table S5). The longest isoform (*PDE8B1*) encodes a protein of 885 amino acids containing an N-terminal REC (cheY-homologous receiver) domain, a PAS (Per, Arnt, and Sim) domain, and a C-terminal catalytic PDE domain (Figure 2D).[3] The functions of the PAS and the REC domains in PDE8B are unknown.[4] Isoforms 2 and 3 lack part of the PAS domain, but all isoforms contain the REC and the catalytic PDE domain. The REC, PAS, and PDE domains show very high interspecies amino acid conservation (human versus mouse: 98.6%), suggesting an important function of these domains.

The ADSD-causing mutation results in a loss of all three functional domains of PDE8B (Figures 2D and 2E), which most likely causes a complete loss of function of the truncated protein. To prove the loss of phosphodiesterase enzymatic activity of mutated PDE8B, we transfected COS-7 cells with isoform 1 of wild-type *PDE8B* (pEGFP-PDE8BWt), mutated *PDE8B* (pEGFP-PDE8B-Mut), or empty vector (pEGFP). COS-7 cells were cultivated in Dulbecco's

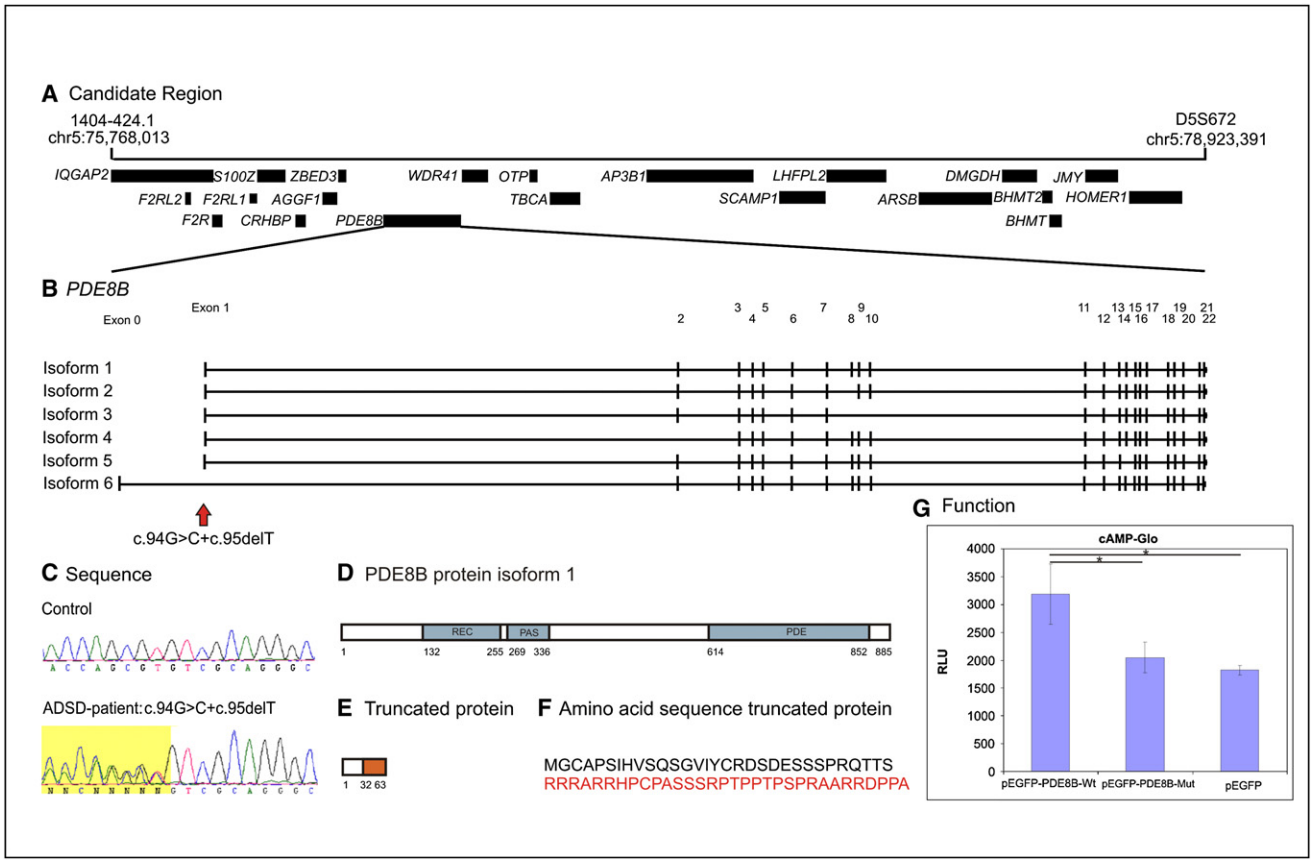

Figure 2. ADSD Candidate Region, Genomic Organization of *PDE8B*, *PDE8B* Mutation Found in the ADSD Family, Structural and Functional Consequences for the Protein

(A) The 3.25 Mb candidate region with locations of all 21 RefSeq annotated protein coding genes.
(B) Genomic organization of the different *PDE8B* variants. The localization of the ADSD-causing mutation in exon 1 is indicated by an arrow. Accession numbers of *PDE8B* isoforms are given in Table S4.
(C) Complex (c.94G>C+c.95delT) mutation found in the ADSD family. Shown is the reverse sequence.
(D) Protein structure of PDE8B and position of the functional domains REC, PAS, and PDE in PDE8B isoform 1.
(E) Structure of the truncated protein. The altered amino acid sequence starting at residue 32 is shaded.
(F) Amino acid sequence of the truncated protein. Residues 1–31 (upper row, black) and altered residues 32–63 (lower row, red) are shown.
(G) Effects of the *PDE8B* mutation on cAMP levels. All error bars indicate standard deviation (SD). Each sample was run in triplicate ($n = 3$) and the experiment was repeated three times. * indicates a significant difference between wild-type and mutant ($p < 0.05$) and wild-type and empty vector ($p < 0.01$). The difference between mutant and empty vector was not significant. Luminescence (RLU) is inversely proportional to cAMP levels. High PDE8B activity results in low cAMP concentration, leading to high luminescence.

modified Eagle's medium high glucose with L-Glutamine and with sodium pyruvate (Th. Geyer) supplemented with 5% fetal calf serum (Invitrogen) and 1% Pen/Strep-Premix (Carl-Roth) at 37°C with 5% CO_2. Transfections were performed with either Turbofect (Fermentas) or Nanofect (PAA Laboratories) according to the manufacturers' recommendations. A full open reading frame clone containing wild-type *PDE8B* isoform 1 was obtained from Imagenes. The ADSD-causing mutation (c.94G>C+c.95delT) was introduced with the QuickChange XL Site-Directed Mutagenesis Kit (Stratagene). Wild-type and mutant *PDE8B* were PCR amplified via primers containing HindIII and *EcoR1* sites. The PCR products were subcloned into pEGFP-N3 (Clontech) to generate constructs expressing PDE8B C-terminally fused to enhanced green fluorescent protein (EGFP). The inserts of all constructs were verified by DNA sequencing.

Quantitative determination of cAMP was carried out via the cAMP-Glo Assay (Promega). A total of 20,000 COS-7 cells were grown in poly-D-lysine-coated, white, clear-bottom, 96-well plates (Nunc). After 24 hr, the cells were transfected with 0.2 μg of plasmid. Then, 24 hr after transfection, cells were incubated with induction buffer (2000 μM IBMX), 400 μM 4-(3-butoxy-4-methoxybenzyl) imidazolidone (Ro 20-1724), and 18 μM Forskolin (all from Sigma-Aldrich) in PBS, pH 7.4 (Invitrogen) for 30 min at 37°C. The assay was performed according to the recommendations of the manufacturer. Luminescence was measured with a TRIAD plate reader (Dynex Technologies).

All experiments were performed three times, and each sample was run in triplicate ($n = 3$). Error bars indicate standard deviations. Statistical differences were determined by one-way analysis of variance with Bonferroni correction

for multiple testing. Statistical significance was assumed at $p < 0.05$.

Although overexpressing wild-type PDE8B in COS-7 cells significantly reduced cAMP levels compared to the empty vector control, mutated PDE8B was not distinguishable from empty vector (Figure 2G). Protein expression levels were determined qualitatively by immunoblot analysis. COS-7 cells were seeded in 6 well plates (80×10^3 per well) and transfected after 24 hr with 2.5 μg plasmid DNA. Cells were lysed in SDS buffer. After measuring protein concentration, 50 μg of protein lysate was run on a 10% SDS gel. The gels were blotted onto a polyvinylidene fluoride (PVDF) membrane incubated with the antibodies after blocking. Polyclonal anti-GFP antibody (Invitrogen) was used in a 1:2000 dilution. The blot was then incubated with horseradish conjugated goat anti-rabbit antibody (Bio-Rad) diluted 1:30,000. SuperSignal West Pico Substrate Kit (Fisher Scientific) was used as chemiluminescent substrate. Signals were detected via a Chemoluminescence Imager (Biozym). Immunoblotting demonstrated that the expression levels of wild-type PDE8B were consistently lower than those of mutant PDE8B (Figure S1A). Therefore, the difference in enzymatic activity between wild-type and mutant PDE8B is underestimated in our analysis. As expected, the ADSD-causing mutation results in a loss of phosphodiesterase activity.

PDE8B expression has been reported in thyroid gland, brain, placenta, pancreas, and adrenal cortex.[4,5] Previous studies suggest that PDE8B expression is higher in brain regions affected by ADSD (caudate nucleus and putamen) than in most other regions of the brain (e.g., cerebellum).[6] To confirm and extend these findings, we assessed *PDE8B* expression in different human tissues by quantitative real-time PCR (qPCR). RNA was either purchased (Clontech) or isolated with Trizol (Invitrogen) or the RNeasy Mini Kit (QIAGEN). RNA was reverse transcribed with the QuantiTect Reverse Transcription Kit (QIAGEN). *PDE8B* primers were as follows: forward, 5′-CTGTGGTGATGCCA GTGTT-3′; and reverse, 5′-TTGTCAGCCAAATGTTGCAT-3′. qPCR was performed in a total reaction of 25 μl with 2× HotStart PCR MasterMIX including SYBR Green I (KSI) according to the manufacturers recommendations. qPCR data were obtained with a Rotor-Gene 3000 instrument (Corbett Research, LTF-Labortechnik). At the end of each run, a melting curve analysis was performed to assess nonspecific signals. Each sample was run in triplicate, and the means were used for further calculations. Relative mRNA levels were quantified via the comparative C_T method. For normalization we used the geometric mean of three internal control genes: beta-actin (*ACTB* [MIM 102630]), glyceraldehyde-3-phosphate dehydrogenase (*GAPDH* [MIM 138400]), and peptidyl-prolyl isomerase a (*PPIA* [MIM 123840]). Reference gene primers were obtained from Promolgene. We showed that *PDE8B* expression is higher in putamen than in pallidum and total brain. The putamen belongs to the striatum, which is affected by ADSD. Peripheral tissues (adrenal gland, liver, skeletal muscle, skin fibroblasts, leukocytes) showed a much lower *PDE8B* expression (Figure 3).

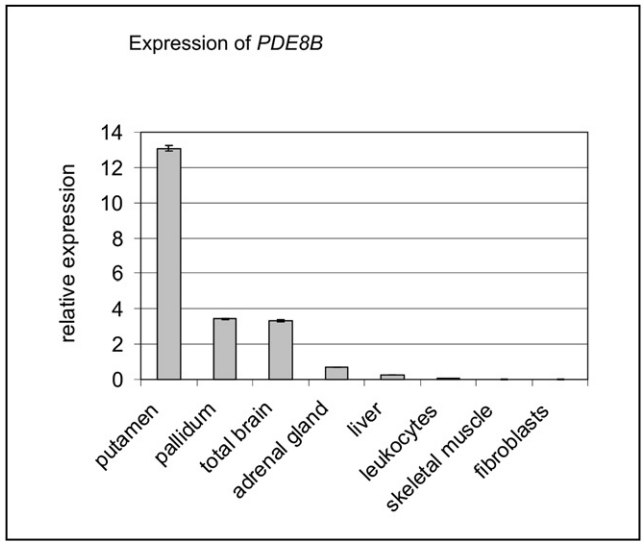

Figure 3. Expression of *PDE8B*
Relative quantification of *PDE8B* in various human tissues by real-time PCR and standard deviation. Quantification was performed with *ACTB*, *GAPDH*, and *PPIA* as reference genes. All error bars indicate SD. Each sample was run in triplicate (n = 3).

In addition, we carried out qualitative RT-PCR for the *PDE8B* isoforms in different brain regions. Primer sequences are given in Table S6. Isoforms 2–6 are present in putamen, pallidum, and total brain (Figure S1B). Because isoform 1 contains no unique DNA sequences that are not also present in other isoforms, it cannot be amplified by RT-PCR without coamplifying other isoforms. Therefore, its expression cannot be analyzed separately by RT-PCR. In ADSD patients, all functional domains of PDE8B are lost in isoforms 1–5 (Figures 2B, 2D, and 2E). Isoform 6 starts with an alternative first exon. Therefore, its amino acid sequence remains unaffected by the mutation (Figure 2B).

To analyze the cellular localization of wild-type PDE8B protein versus mutant PDE8B protein, we generated a wild-type PDE8B expression vector tagged with cherry red fluorescent protein (pCherry-PDE8BWt) in addition to the above-mentioned GFP-tagged constructs. pCherry is a derivative of pEGFP-N3, in which we exchanged EGFP for cherry fluorescent protein. Next we performed single transfections and cotransfections of NIH 3T3 and HEK293 cells with pEGFP-PDE8BMut and pCherry-PDE8BWt constructs and compared the subcellular localization via confocal microscopy. NIH 3T3 and HEK293 cells were grown on coverslips and transfected as described above. Cells were methanol fixed 24 hr after transfection, stained with DAPI (Roche), and mounted with Immumount (Fisher Scientific). Images were acquired with a confocal laser-scanner microscope (Zeiss LSM 510). We did not observe any difference in the localization of wild-type versus mutant protein (Figure S1C). The localization of PDE8B wild-type and mutant clearly differed from that

of an empty vector control, which was diffusely distributed across the cytoplasm (data not shown). However, the localization of the small mutated PDE8B protein might be severely influenced by the large fused fluorescent protein, limiting the value of this analysis.

In summary, we show that a complex mutation in *PDE8B* resulting in a frameshift leading to a severely truncated, dysfunctional protein causes ADSD. ADSD is characterized by dysfunction and morphological changes of the striatal part of the basal ganglia. PDE8B could play an important role in the regulation of neuronal function, especially in the striatum. PDE8B regulates cAMP levels and therefore might influence the dopaminergic neurotransmission in the striatum. Five subtypes of dopamine receptors (*DRD1-5* [MIM 126449-126453]) have been described.[7] *DRD1* and *DRD2* receptors are highly expressed in the striatum.[8] *DRD1* and *DRDR5* receptors stimulate cAMP synthesis and form the D1-like receptor family. Receptors *DRD2*, *DRD3*, and *DRD4* inhibit cAMP synthesis and constitute the D2-like receptor family. Parkinson disease is characterized by a lack of dopamine in the brain and an excellent therapeutic response to L-Dopa. In contrast, ADSD patients do not show a good L-Dopa response. Taking into account that PDE8B degrades cAMP, the second messenger of dopamine receptors, one might speculate that ADSD is caused by a defect in dopamine signaling downstream of the dopamine receptors.

Elucidating the causative genetic defects of monogenic forms of common polygenic diseases and related disorders has contributed eminently to understanding the pathomechanisms underlying Parkinson disease and other related neurological disorders.[9,10] We believe that the functional analysis of *PDE8B* will help to elucidate the pathomechanism of ADSD and will contribute to our understanding of other related neurological disorders.

Supplemental Data

Supplemental Data include one figure, six tables, and one movie and can be found with this article online at http://www.ajhg.org.

Acknowledgments

The authors are grateful to the patients and their relatives who participated in this study. The VIB Genetic Service Facility contributed technically to the genetic analyses. This work was supported by grants from the Cluster of Excellence "Inflammation at Interfaces" of the Christian-Albrechts University of Kiel, the Ministry for Science, Economics and Transport of Schleswig-Holstein, the Innovative Medizinische Forschung of the University of Münster (KU110004), the Deutsche Forschungsgemeinschaft (KU1194/3-1), and the Heinrich-Hertz Foundation (B42, 15/03) to G.K., and by a Methusalem grant of the University of Antwerp, the Fund for Scientific Research (FWO-Flanders), the Medical Foundation Queen Elisabeth (GSKE), and the Interuniversity Attraction Poles P6/43 program of the Belgian Federal Science Policy Office (BELSPO) to P.D.J and V.T. We thank Heiner Nattkämper, Marcus Lettau, Els De Vriendt, Sabine Weiser, and May Bungeroth for technical support.

Received: October 28, 2009
Revised: December 3, 2009
Accepted: December 8, 2009
Published: January 7, 2010

Web Resources

The URLs for data presented herein are as follows:

NCBI SNP Database (dbSNP), http://www.ncbi.nlm.nih.gov/projects/SNP
UCSC Human Genome Browser, March 2006 build, http://www.genome.ucsc.edu/cgi-bin/hgGateway
Online Mendelian Inheritance in Man (OMIM), http://www.ncbi.nlm.nih.gov/Omim

References

1. Kuhlenbäumer, G., Lüdemann, P., Schirmacher, A., De Vriendt, E., Hünermund, G., Young, P., Hund-Georgiadis, M., Schuierer, G., Möller, H., Ringelstein, E.B., et al. (2004). Autosomal dominant striatal degeneration (ADSD): Clinical description and mapping to 5q13-5q14. Neurology *62*, 2203–2208.
2. Bender, A.T., and Beavo, J.A. (2006). Cyclic nucleotide phosphodiesterases: Molecular regulation to clinical use. Pharmacol. Rev. *58*, 488–520.
3. Gamanuma, M., Yuasa, K., Sasaki, T., Sakurai, N., Kotera, J., and Omori, K. (2003). Comparison of enzymatic characterization and gene organization of cyclic nucleotide phosphodiesterase 8 family in humans. Cell. Signal. *15*, 565–574.
4. Hayashi, M., Shimada, Y., Nishimura, Y., Hama, T., and Tanaka, T. (2002). Genomic organization, chromosomal localization, and alternative splicing of the human phosphodiesterase 8B gene. Biochem. Biophys. Res. Commun. *297*, 1253–1258.
5. Horvath, A., Giatzakis, C., Tsang, K., Greene, E., Osorio, P., Boikos, S., Libè, R., Patronas, Y., Robinson-White, A., Remmers, E., et al. (2008). A cAMP-specific phosphodiesterase (PDE8B) that is mutated in adrenal hyperplasia is expressed widely in human and mouse tissues: A novel PDE8B isoform in human adrenal cortex. Eur. J. Hum. Genet. *16*, 1245–1253.
6. Hayashi, M., Matsushima, K., Ohashi, H., Tsunoda, H., Murase, S., Kawarada, Y., and Tanaka, T. (1998). Molecular cloning and characterization of human PDE8B, a novel thyroid-specific isozyme of 3′,5′-cyclic nucleotide phosphodiesterase. Biochem. Biophys. Res. Commun. *250*, 751–756.
7. Missale, C., Nash, S.R., Robinson, S.W., Jaber, M., and Caron, M.G. (1998). Dopamine receptors: From structure to function. Physiol. Rev. *78*, 189–225.
8. Levey, A.I., Hersch, S.M., Rye, D.B., Sunahara, R.K., Niznik, H.B., Kitt, C.A., Price, D.L., Maggio, R., Brann, M.R., Ciliax, B.J., et al. (1993). Localization of D1 and D2 dopamine receptors in brain with subtype-specific antibodies. Proc. Natl. Acad. Sci. USA *90*, 8861–8865.
9. Dekker, M.C., Bonifati, V., and van Duijn, C.M. (2003). Parkinson's disease: Piecing together a genetic jigsaw. Brain *126*, 1722–1733.
10. Krüger, R., Eberhardt, O., Riess, O., and Schulz, J.B. (2002). Parkinson's disease: one biochemical pathway to fit all genes? Trends Mol. Med. *8*, 236–240.